Title	On the Relation between Surface-Wave Magnitude and JMA magnitude
Author(s)	NOGUCHI, Shin'ichi
Citation	Journal of the Faculty of Science, Hokkaido University. Series 7, Geophysics, 6(1), 213-224
Issue Date	1980-03-31
Doc URL	http://hdl.handle.net/2115/8716
Type	bulletin (article)
File Information	6(1)_p213-224.pdf

[Journal of the Faculty of Science, Hokkaido University, Ser. VII (Geophysics), Vol. VI, No. 1, 1979]

On the Relation between Surface-Wave Magnitude and JMA Magnitude

Shin'ichi NOGUCHI

(Received Oct. 16, 1979)

Abstract

The relation between the surface-wave magnitude M_S and the JMA magnitude M_J is investigated on the basis of the observations of more than two hundred earthquakes of $M_S=4.0$ to 8.0. M_S versus M_J relation for small earthquakes is considerably different from that for large ones in spite of the fact that M_J was calibrated for M_S. The difference between M_J and M_S decreases systematically with increase of M_S in the range of M_S of about 5.0 to 6.5. Below M_S 5.0, M_J is larger by about 0.6 on the average than M_S, while for $M_S=6.5$ or more, M_J is smaller by about 0.1 on the average than M_S. M_J is found to be determined at a period of about 3 sec independent of magnitude. The difference between M_S and M_J is investigated constructing a theoretical M_S versus M_J relation based on a fault model. The observed M_S versus M_J relation for $M_S<6.5$ is explained well by the theoretical relation. A faulting mechanism which emphasizes an efficient radiation of short-period seismic waves is suggested for $M_S>6.5$. It is concluded that M_J of a large earthquake represents a magnitude of partial fault breakings rather than one entire rupture.

1. Introduction

Although magnitude is the most commonly used parameter in constraining the size of an earthquake, several magnitude scales currently used are not consistent with each other for an earthquake. For many earthquakes occurring in and around Japan, the magnitudes are determined on a routine basis by Japan Meteorological Agency (JMA). The magnitude formula adopted by JMA was originally defined by Tsuboi[1], who adjusted amplitude data observed at six stations in Japan for 78 earthquakes to the Gutenberg-Richter's[2] magnitude in "Seismicity of the Earth". Since the Gutenberg-Richter's magnitude of large earthquakes in "Seismicity of the Earth" are supposed to be essentially equivalent to the 20-sec surface-wave magnitude M_S[3], it is natural that JMA magnitude scale corresponds linearly to M_S scale. Recent investigations by Katsumata and Kashiwabara[4], however, showed that for small earthquakes, the JMA magnitude M_J correspond to the body-wave magnitude m_b rather than M_S. They also suggested that the M_S versus M_J relation for small earthquakes is different from that for large ones. Direct comparison between M_S and M_J for small earthquakes have not been sufficiently tried as yet, because M_S for small events are scarcely determined.

In view of the basic importance of M_J scale in various field in Japan, it is necessary to know the exact relation between M_S and M_J scale in the wide range of magnitude. In this paper, we compare M_S with M_J for more than two hundred of earthquakes including small ones. In order to determine M_S, we measure a number of amplitudes and periods of surface-waves recorded by long-period seismographs at many stations in the world. To explain the observed M_S vs. M_J relation, theoretical M_S vs. M_J relation is discussed in terms of earthquake source theory.

2. M_S determination

Fig. 1 shows the epicenter distribution of shallow earthquakes for which the M_S vs. M_J relation is investigated. About two hundred of earthquakes are plotted on the map, most of them are concentrated along the Kurile-Kamchatka, North-eastern Japan, Izu-Ogasawara and Ryukyu trenches.

For the determination of M_S, we used the formula proposed by Vaněk *et al.*[5)]

$$M_S = \log\left(\frac{A}{T}\right)_{\max} + 1.66 \log \Delta + 3.3 \tag{1}$$

where Δ is the epicentral distance in degrees, A is the displacement amplitude in microns, and T is the corresponding period in seconds. A and T are measured in the wave group that gives the maximum of A/T. Since the above formula was introduced for a period of about 20 sec, the measurement of A and T was made for the period range 17 to 23 sec. Epicentral distance was restricted 20 to 160 degrees.

The amplitude A in equation (1) is defined as the combined horizontal amplitude:

$$A = A_H = (A_N{}^2 + A_E{}^2)^{1/2} \tag{2}$$

where A_N and A_E are the maximum amplitude on the N-S and E-W component, respectively. Since the vertical broad-band instrument came extensively into practical use, only vertical component, A_V, has been in general use in equation (1). Earthquake Data Reports (EDR) have reported M_S since

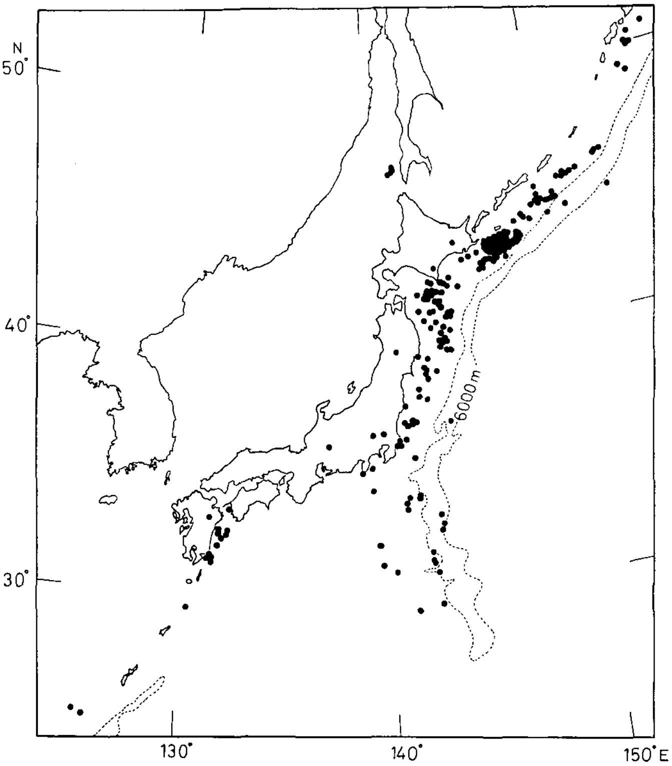

Fig. 1 Epicenters of earthquakes in and around Japan for which the M_S versus M_J relation is investigated.

1968 using equation (1) and horizontal amplitude A_H, then in mid 1975, EDR exchanged A_H to A_V[6]. In practical use of A_V instead of A_H, it is necessary to know previously whether A_V is comparable to or larger than A_H.

We examined the relation between A_H and A_V. About 350 A_H vs. A_V were obtained for 20 earthquakes in the magnitude range of M_S 5.0 to 7.7 using many seismograms from the Worldwide Standardized Seismograph Network (WWSSN). The result are shown in Fig. 2a and 2b. From Fig. 2a, it is evident that A_H and A_V has a linear relation. Fig. 2b shows the histogram of $\log(A_V/A_H)$. Most of them are within ±0.3 and the peak of the histogram is at $\log(A_V/A_H)=0.0$.

Based on these observational results we can safely conclude that A_H is empirically equivalent to A_V on the average. This result is consistent with

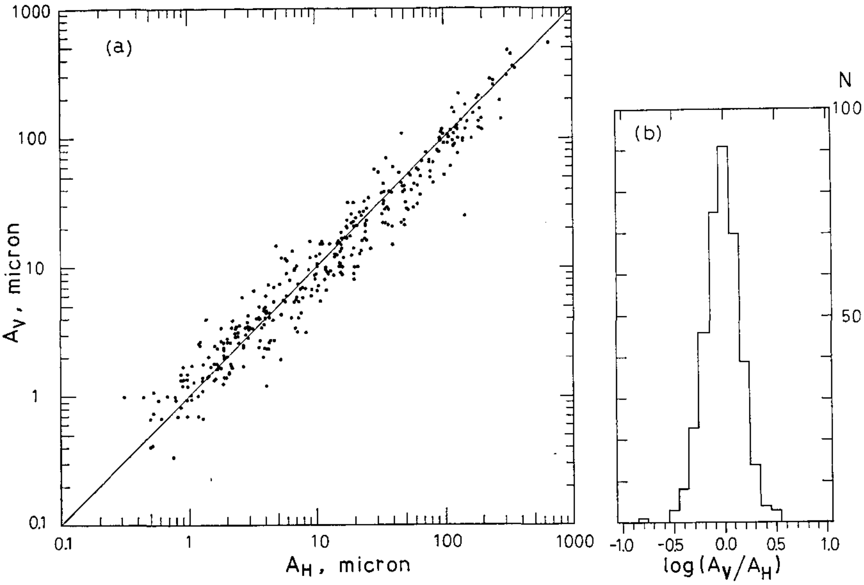

Fig. 2 Relation between the vector sum of horizontal component amplitude A_H and vertical component amplitude A_V. (*a*): About 350 data are plotted for 20 earthquakes of M_S 5.0 to 7.7. (b): Histogram of $\log(A_V/A_H)$.

the investigations by Gorbunova *et al.*[7] and Båth[8]. Considering these results, we hereafter use only vertical component in computing M_S instead of horizontal component.

Fig. 3 shows the examples of surface-wave seismograms of a small aftershock of the Southern Kurile island earthquake of 1975, recorded by the WWSSN long-period instruments at Quetta, Pakistan. The predominant period of the surface-waves is about 20 sec. M_S was determined to be 4.3 as the average of ten WWSSN stations, most of them having instrumental magnifications of either 3,000 or 6,000; for smaller shocks the amplitudes are too small to register except near distance stations. In order to determine M_S of these smaller events, we supplemented records from high-gain long-period networks. Bulletin of International Seismological Center (ISC) and EDR were used when the reported amplitudes and periods are available.

3. Observed M_S versus M_J relation

Fig. 4 shows the relation between M_J-M_S and M_S for a total of 205 earthquakes in and around Japan during the period from 1964 to 1978.

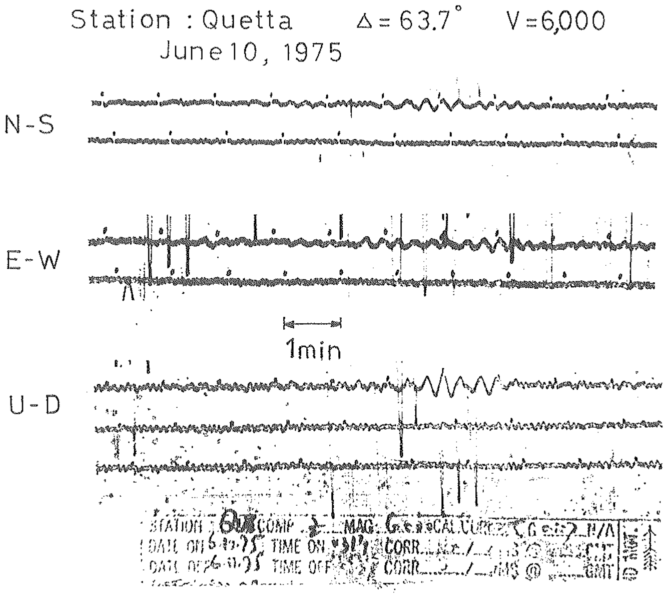

Fig. 3 An example of surface-waves for a small earthquake recorded on long-period instruments with a magnification of 6,000 at Quetta Pakistan.

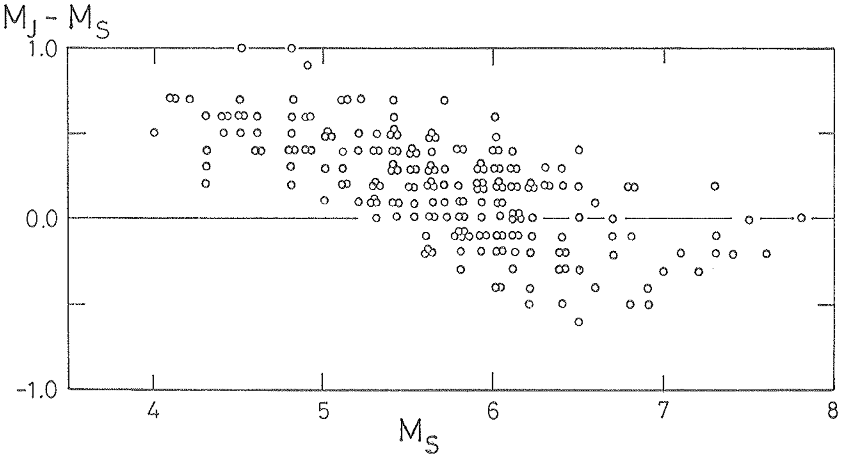

Fig. 4 Comparison between M_S and M_J-M_S for 205 earthquakes.

Five or more stations are always used for determination of M_S of each event. The standard deviations are generally about ±0.3. M_J are taken from The Seismological Bulletin of JMA. According to the note of the Bulletin[9), M_J is determined through the Tsuboi's[1) formula:

$$M_J = \log (A_N{}^2 + A_E{}^2)^{1/2} + 1.73 \log D - 0.83 \qquad (3)$$

where A_N and A_E are the maximum ground amplitude of N-S and E-W component in microns with a period less than five seconds, respectively. D is the epicentral distance in kilometers.

Fig. 4 represents systematic decrease of M_J-M_S with increase of M_S. Especially, variations of M_J-M_S in the range of M_S 5.0 to 6.5 are significant.

One important subject we must take into account here is the detection threshold for both M_S and M_J for small events. For M_J, Mochizuki *et al.*10) have investigated the smallest magnitude for which the every hypocenter can be determined by JMA seismological observation system. According to the result, the smallest M_J is about 4.0 for inland earthquakes and is about 4.3 to 5.3 for off-shore events occurring around Japan.

For M_S, M_S can not be determined for all the events for which M_J are determined. For an event with M_S as small as 4.3, M_S can be clearly detected by the WWSSN and the high-gain long-period instruments as shown in Fig. 3. If there were an event with M_S larger than M_J for $M_S < 5.0$, the surface-wave could be enoughly detected, but such an event was not found at all. The range of M_S for which the systematic change of M_J-M_S was observed are about 5.0 to 6.5 (Fig. 4), and this range are sufficiently larger than the detection threshold for M_S and M_J.

From above considerations, it is concluded that the important feature found is not due to the artificial effect of the detection threshold for small events.

The relation between the magnitude and the seismic source spectrum has been discussed within a framework of an earthquake source theory11). It is reasonable to assume that the magnitude scale is proportional to the logarithm of the seismic source spectral density at the period where the magnitude is determined. If it is true, the observed M_S vs. M_J relation seems to reflect a different part of seismic source spectrum. For a detailed discussion of the observed M_S vs. M_J relation, we will next construct the seismic source spectrum and derive the theoretical M_S vs. M_J relation.

4. Seismic source spectrum and theoretical M_S versus M_J relation

Though simple, Haskell's[12] dynamic fault model has been used successfully to explain the gross relations between the seismic source parameters of large and great earthquakes[13],[14]. This model is also useful to explain the observed M_S vs. m_b relation in terms of dynamic process of earthquake faulting[15]. Since the method of calculating theoretical source spectrum and various scaling relations between the magnitudes and source parameters were described in Noguchi and Abe[15], we use their results for deriving the theoretical M_S vs. M_J relation.

The average far-field seismic spectra are shown in Fig. 5. The fault length is an independent parameter of source size. The decay form of the high frequency spectra in Fig. 5 shows a gradual transition from ω^0 to ω^{-3}, where ω is an angular frequency corresponding to three corner frequencies; the finite effects of fault length, width and dislocation time function. This differs from Aki's[11] ω-cube model which has a single corner frequency.

For the theoretical M_S, it is assumed that M_S is defined as follows:

$$M_S = \log A_{20} + C_{M_S} \tag{4}$$

where A_{20} is the displacement spectral density at 20 sec and C_{M_S} is the additive constant. The constant was determined to be $C_{M_S}=2.88$ so that $\log A_{20}$ saturates at $M_S=8.22$[14], because for great earthquakes the 20-sec surface-waves become to saturate around this size. M_S values calculated from equation (4) are plotted on the curves in Fig. 5.

In the calculation of M_J, the period is not exactly defined. We examined the average period at which M_J has been determined. The periods of the maximum amplitude of both N-S and E-W components listed in The Seismological Bulletin of JMA were examined. An average value of 2.8±0.7 sec was determined from more than 800 data with periods less than 5 sec for 34 earthquakes of M_J 4.3 to 7.9. Some systematic increase of the period with the increase of M_J was recognized; about 2.0 sec for $M_J=4$ class and about 3.5 sec for $M_J=7$ class events. Its increment, however, is very small.

Thus it can be assumed that M_J is determined at the period of about 3 sec. Since the coefficient of log amplitude in equation (3) is unity, the theoretical M_J can be approximated as follows:

$$M_J = \log A_3 + C_{M_J} \tag{5}$$

where A_3 is the displacement spectral density at 3 sec and C_{MJ} the additive

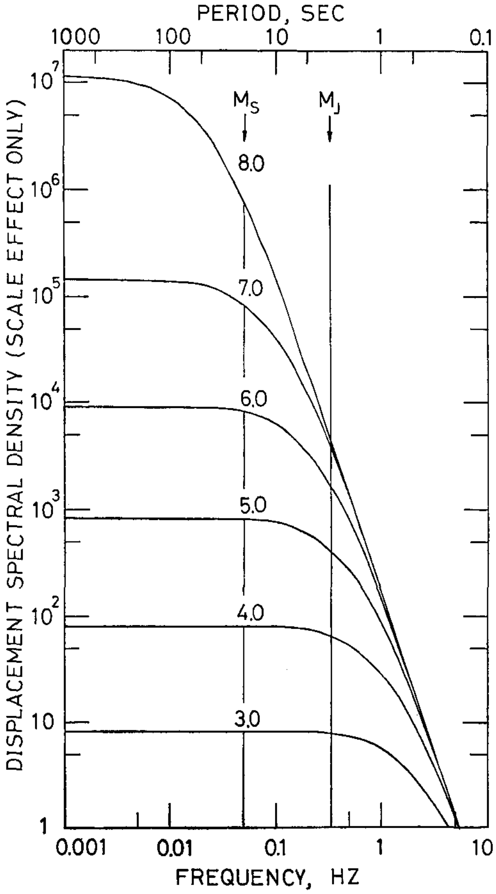

Fig. 5 Far-field seismic spectral density as a function of M_S. Theoretical M_J is defined at a period of 3 sec.

constant. The constant was determined to be $C_{MJ}=3.80$ so that M_J agrees with M_S at 6.0. Once the theoretical M_S and M_J are defined, their relation can be obtained by using an independent source parameter, that is fault length.

The curve in Fig. 6 shows the theoretical relation between M_J-M_S and M_S. Averages and standard deviations of the observed M_J-M_S over 0.6 M_S intervals are also plotted. It can be seen that the theoretical curve fits well with the average M_J-M_S for small earthquakes. As mentioned before, for the theoretical M_J, the additive constant C_{MJ} was chosen so that M_S and M_J agree at 6.0. The constant C_{MJ} does not affect the theoretical curve at all, it only shifts up and down. Thus the systematic decrease of observed M_J-M_S with increase of M_S can be attributed to the relatively less efficient radiation of the short-period seismic waves than that of the long-period, with the increase of the fault dimension. For large events of $M_S=6.5$ or more, the theoretical curve is deviated from the observed data; observed M_J-M_S show that a few seconds seismic waves are radiated to be proportional to the 20-sec surface-waves. These features are very important for understanding the characteristics of M_J scale. Furthermore, the good agreement of the theoretical M_S vs. M_J with observed data for $M_S<6.5$ and the discrepancy for larger shocks imply different scaling relations between large and small earthquakes.

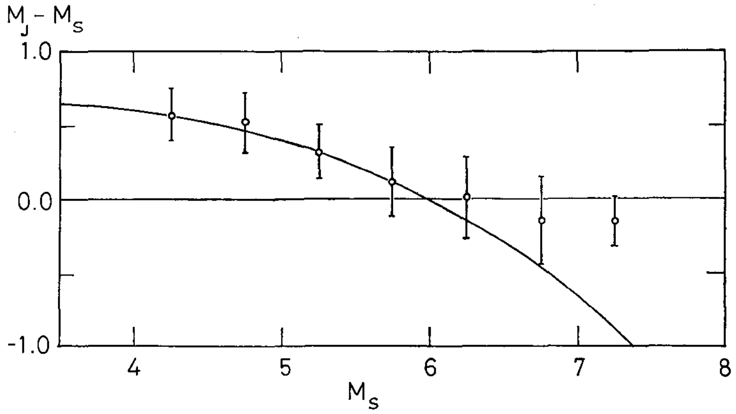

Fig. 6 Comparison of average M_J-M_S versus M_S with theoretical one calculated from the source spectral density shown in Fig. 5.

5. Discussion and conclusion

Direct comparison between M_S and M_J in the wide range of magnitude (about M_S 4.0 to 8.0) revealed that there is a considerable discrepancy between M_S and M_J, especially for small earthquakes. The average value of M_J-M_S is $+0.55$ for $M_S<5.0$, and -0.14 for $M_S>6.5$. The systematic change of M_S vs. M_J relation for $M_S<6.5$ is explained well by the theoretical M_S vs. M_J relation based on a simple fault model, while for $M_S>6.5$, the theoretical relation is not consistent with the observed data.

We consider here a faulting mechanism which emphasizes a more efficient radiation of a few seconds seismic waves for $M_S>6.5$. It seems unlikely that the crustal structure is homogeneous over the whole rupture area of a large earthquake. If multiple shocks occur discretely at equally spaced segments in the framework of Haskell's[12] fault model, a spectral peak appears at a short period corresponding to the time interval of each rupture. The appearance of a spectral peak around a few seconds corresponds to a interval of about 10 km, assuming a rupture velocity of about 3 km/sec. This estimate suggests a segmental fracture of an earthquake with M_S larger than 6.0. It is also considered that the radiation of a few seconds seismic waves is affected by regional difference of stress release. Intraplate earthquakes in the Japanese Islands have relative high stress drop compared with large interplate shocks and the complete release of effective stress[16),17),18),19),20)]. M_S and M_J of inland and near-coast earthquakes are listed in Table 1. M_J-M_S of these earthquakes is systematically larger than that of interplate shocks, which suggests that these earthquakes have a higher stress drop than that of interplate shocks. From these observation and theoretical consideration, it can be said that a large earthquake with $M_S>6.5$ consists of fault segments, some of which have higher stress drop than the average over the whole rupture area, and M_J represents a magnitude of the local fault breakings.

Table 1. M_S and M_J of inland and near-coast earthquakes.

Date	Time	Location		Region	M_J	M_S	N
	(JMT)	E	N				
1967 Nov. 4	23:30	144.3	43.5	E PART OF HOKKAIDO	6.5	6.0	5
1968 July 1	19:45	139.4	36.0	MIDDLE OF SAITAMA PREF	6.1	5.4	6
1968 Aug. 6	01:17	132.4	33.3	W COAST OF EHIME PREF	6.6	6.3	6
1969 Sep. 9	14:15	137.1	35.8	MIDDLE OF GIFU PREF	6.6	6.0	5
1970 Jan. 21	02:33	143.1	42.4	S PART OF HOKKAIDO	6.7	6.4	13
1970 Oct. 16	14:26	140.8	39.2	SE AKITA PREF	6.2	5.8	9
1974 Mar. 3	13:50	140.9	35.6	E OFF CHIBA PREF	6.1	5.6	8
1974 May 9	08:33	138.8	34.6	NEAR S COAST OF IZU PEN	6.9	6.5	11
1975 Jan. 23	23:19	131.1	33.0	NE KUMAMOTO PREF	6.1	5.6	4
1975 Apr. 21	02:35	131.3	33.1	CENTRAL OITA PREF	6.4	5.7	7

N: the number of stations used to determine M_S.

We were concerned mainly with amplitudes and periods as the most important factors which control the M_S vs. M_J relation. Matsumoto[21] has suggested that the coefficient of log D in equation (3) for small earthquake is different from that for large one. This is based on Wadati's[22] investigation of the relation between the maximum ground amplitude and the epicentral distance for shallow earthquakes near Japan. He found that the smaller the size of the earthquake is, the more rapidly the amplitude decreases with increase of distance. In actual, however, equation (3) is used for the limited range of periods independent of magnitude. In this case the effect of the coefficient is not important in explaining the difference between M_S and M_J.

The results obtained here can be summarized as follows: (1) M_J determined from the vertical component is essentially equivalent to M_S from the combined horizontal amplitude in the wide range of magnitude. (2) M_S vs. M_J relation for 205 earthquakes showed that M_S vs. M_J relation for small earthquakes is considerably different from that for large ones. The average of M_J-M_S is $+0.6$ for $M_S<5.0$, and is -0.1 for $M_S>6.5$. This difference can be explained partially in terms of an earthquake source theory. (4) JMA magnitude is determined at a relatively short period of about 3 sec, and M_J for large earthquakes is considered to represent a magnitude of partial fault breakings rather than one entire rupture. (5) It is suggested that the difference between M_S and M_J will be associated with the dynamic process of the stress release and the mode of local fault breakings.

Acknowledgements: I wish to express my gratitude to Professors Izumi Yokoyama and Katsuyuki Abe for their continuing guidance and encouragement. I am very grateful to Professor Katsuyuki Abe for critical review and many valuable suggestions on which the manuscript was greatly improved. I am also grateful to Dr. Hiromu Okada for kindly reading the manuscript and for providing me useful Russian papers on magnitude.

References

1) TSUBOI, C.: Determination of the Gutenberg-Richter's magnitude of earthquakes occurring in and around Japan. Zisin, II, **7**, (1954) 185–193, (in Japanese).
2) GUTENBERG. B. and C.F. RICHTER: Seismicity of the Earth and Associated Phenomena. 2nd. ed., Princeton Univ. Press, (1954).
3) GELLER, R.J. and H. KANAMORI: Magnitudes of great shallow earthquakes from 1904 to 1952. Bull. Seism. Soc. Am., **67**, (1977) 587–598.
4) KATSUMATA, M. and S. KASHIWABARA: Note on JMA magnitude scale. Zisin, II, **30**, (1977) 511–513, (in Japanese).
5) VANĚK, J., A. ZÁTOPEK, V. KÁRNIK, N.V. KONDORSKAYA, Y.V. RIZNICHENKO, E.F. SAVARENSKY, S.L. SOLOV'EV and N.V. SHEBALIN: Standardization of magnitude scales. Bull. Acad. Sci. U.S.S.R., Geophys. Ser., **2**, (1962) 108–111.
6) ABE, K. and H. KANAMORI: Magnitudes of great shallow earthquakes from 1953 to 1977. Tectonophysics, **60**, (1979), (in press).
7) GORBUNOVA, I.V., A.I. ZAKHAROVA and L.S. CHIPKUNAS: Magnitudes M_{LH} and M_{LV}. In: Magnitude and Energy Classification of Earthquakes, Vol. 2, Inst. Phys. Earth, Acad. Sci. U.S.S.R., Moscow, (1974) 87–93, (in Russian).

8) BÅTH, M.: Teleseismic magnitude relations. Seismol. Inst., Uppsala, Rep. No. 2–79, (1979) 37 pp.
9) The Seismological Bulletin of The Japan Meteorological Agency, Introductory Note.
10) MOCHIZUKI, E., E. KOBAYASHI and M. KISHIO: Hypocenter determination ability of JMA seismological observation system during 1965–1974. Quart. J. Seism., **42**, (1978) 23–30, (in Japanese).
11) AKI, K.: Scaling law of seismic spectrum. J. Geophys. Res., **72**, (1967) 1217–1231.
12) HASKELL, N.A.: Total energy and energy spectral density of elastic wave radiation from propagating faults. Bull. Seism. Soc. Am., **54**, (1964) 1811–1841.
13) KANAMORI, H. and D.L. ANDERSON: Theoretical basis of some empirical relations in seismology. Bull. Seism. Soc. Am., **65**, (1975) 1073–1095.
14) GELLER, R.J.: Scaling relations for earthquake source parameters and magnitude. Bull. Seism. Soc. Am., **66**, (1976) 1501–1523.
15) NOGUCHI, S. and K. ABE: Earthquake source mechanism and M_S-m_b relation. Zisin, II, **30**, (1977) 487–507, (in Japanese).
16) KANAMORI, H.: Determination of effective tectonic stress associated with earthquake faulting, The Tottori earthquake of 1943. Phys. Earth Planet. Inter., **5**, (1972) 426–434.
17) KANAMORI, H.: Mode of strain release with major earthquakes in Japan. Ann. Rev. Earth Planet. Sci., **1**, (1973) 213–239.
18) ABE, K.: Fault parameters determined by near- and far-field data: The Wakasa Bay earthquake of March 26, 1963. Bull. Seism. Soc. Am., **64**, (1974) 1369–1382.
19) ABE, K.: Seismic displacement and ground motion near a fault: The Saitama earthquake of September 21, 1931. J. Geophys. Res., **79**, (1974) 4394–4399.
20) ABE, K.: Static and dynamic fault parameters of the Saitama earthquake of July 1, 1968. Tectonophysics, **27**, (1975) 223–238.
21) MATSUMOTO, T.: On the spectral structure of earthquake waves — Its influence on magnitude scale. Bull. Earthq. Res. Inst., **37**, (1959) 265–277.
22) WADATI, K.: Shallow and deep earthquakes, 3. Geophys. Mag., **4**, (1931) 231–283.